

CFD Analysis of a Fully Developed Turbulent Flow in a Pipe with a Constriction and an Obstacle

C, Diyoke

Mechanical Engineering Department
Enugu State University of Science & Tech.
Enugu, Nigeria

U, Ngwaka

Mechanical Engineering Department
Enugu State University of Science & Tech
Enugu, Nigeria

Abstract—A CFD simulation of water flow across a circular pipe of diameter 78mm and length 860mm having an obstacle and reduced cross section at a point is presented in this study. A fluent CFD software was used to carry out the simulation of the two dimensional fully developed turbulent model of the compressible flow of water across the pipe. The simulation was based on the standard, two-equation k-ε turbulence model of Reynolds Average Navier Stokes (RANS) equation. A uniform inlet velocity is set as the inlet boundary while a pressure of zero Pa is set as the pressure outlet. The simulation was carried out at three flow rates of 8000 cm³/s, 5000 cm³/s and 4000 cm³/s. The results of the CFD simulations were used to understand the effect a sudden obstruction in the flow on the overall total, dynamic and the static pressure across the pipe length. It was found that for the flow rates of 8000 cm³/s, 5000 cm³/s and 4000 cm³/s, the static pressure difference across the pipe was 689kpa, 25.9kpa, 16.4kpa respectively while the dynamic pressure difference was 41 kpa , 15.8kpa, 10.1kpa respectively. The CFD simulation results also showed varying velocity and pressure fields/contours characteristics of turbulent flows. The simulation also presents the pressure and velocity distributions within the water flow, expanding the understanding of the fluid flow characteristics within the pipe

Keywords—CFD, Pressure difference, Velocity, Flow rate

Abbreviations

A_s	Cross Sectional Area of the pipe (m ²)
CFD	Computational fluid dynamics
D, D1	Diameter of the pipe (m)
D ₂	Diameter of the pipe at the reduce cross-section diameters
KE	kinetic energy (j)
P ₁ , P ₂	Pressure upstream and downstream of the plate (Pa)
Q	Volume flow rate (m ³ /s)
R _e	Reynolds number
V	Velocity of flow (m/s)
Nomenclature	
A	Area (m ²)
D	Diameter (m)
ρ	Density of water (kg/m ³)
Re	Reynolds number
V	velocity (m/s)
Latin alphabet	
μ	Viscosity (Ns/m ²)

INTRODUCTION

Depending on application, flow rates in pipes and pressure developed sometimes is undesirable and need to be controlled or measured for accurate billing of customers. This is most likely in pump and valve designs where there is need to control and measure the rate of discharge of water or fluid or the pressure of discharge. As a result of this, the need for pressure/flow rate control becomes imperative. However, this need for pressure/flow rate control in pipes and some other applications has led to a demand in improved valve designs that can control and measure the pressure and flow rate at economical cost and efficiency. Pump and valve designers often times depend on empirical relations and well known principles to develop new products. This method can be time wasting and result in elaborate test requirement with restricted understanding of the factors that can influence performance. With the quick progress in parallel computing and development of commercial codes, CFD has become a key tool in the development of new products. Together with the experiment it allows for a significant reduction of time from the first design through the prototype to the finished product. CFD simulation technique avails the designer the opportunity to simulate and observe in advance the simulated fluid flow paths within the pipe or device being designed [1,2]. Results from the simulation provide detailed flow fields contours, data and performance predictions. The utilization of CFD in pipe flow related problems is of immense advantage in new valve/pump development, design optimization and many other benefits which may include but not limited to [1],[2]

- Reduced time of development and risk
- Minimised Prototyping
- Minimised re-circulation and detachment of flows
- Optimised performance over certain limit of operation
- Enhanced durability, reliability and lower maintenance cost
- Minimised head losses
- Minimised noise, pulsation, and cavitations

The objective of this study is to examine using CFD the pressure difference exerted on a pipe having an obstacle and reduced cross section at a point. For the purpose, the goal is to generate, analyse and explain the pressure and velocity contours, stream lines, radial profiles and fluctuation characteristics of a turbulent water flow through the pipe and subsequently try to validate the model which may be utilized to further develop the design of a valve to control the flow and to predict its performance under simulated real life conditions.

2. THE SIMULATED MODEL OR FLOW METER

The diagram of the simulated flow meter; a water pipe of diameter 78mm with obstruction and reduced cross section is shown fig 1. It works by the principle of differential pressure or pressure difference as a result of mass flow rate or velocity changes. The pressure drop across the pipe is proportional to the square of the flow rate as in equation 1. [3]

$$\frac{P_1 - P_2}{\rho} = \frac{1}{2} \left(\frac{16Q^2}{\pi^2 D_2^2} - \frac{16Q^2}{\pi^2 D_1^2} \right) \quad (1)$$

The flow being a turbulent one is characterized by unsteady eddying motions that are in constant motion with respect to each other. As the cross sectional area of the pipe decreases, the velocity of the fluid increases with the static pressure correspondingly decreasing. According to the laws governing fluid dynamics, a fluid's velocity must increase as it passes through a narrow path to satisfy the principle of continuity [2], whereas its pressure must decrease to satisfy the principle of conservation of mechanical energy. Accordingly the decrease of the cross section of the flowing fluid in passing through the decreased area increases the velocity head at the expense of the pressure head, and the drop in pressure between the plates is measured by a manometer. Measurement of this pressure drop is an indication of the flow rate.

Bernoulli's equation provides a basis for correlating the increase in velocity head with the decrease in pressure head [3] The higher the velocity of the fluid, the higher the pressure difference because at high velocity, the randomness and rapid fluctuations of the swirling fluid particles called eddies increase throughout the flow. These fluctuations lead to higher rate of mixing and turbulence which give rise to high rate of momentum transfer from the fluid to the pipe walls. This then leads to a higher shear stress and pressure drop.

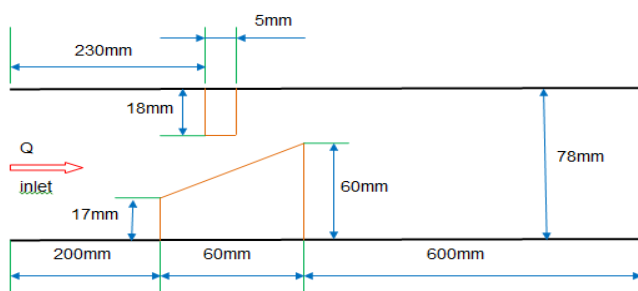


Fig.1: Line Diagram of the simulated pipe

3. SIMULATION METHODOLOGY

3.1 Pre processing

The various dimensions of the pipe model shown in fig. 1 were noted and using the measured dimensions, a meshed structure made up of fine and coarse mesh of the pipe was drawn with the help of GAMBIT which is the pre-processor bundled with FLUENT. Then the meshed structure was exported as the mesh file and was analyzed with proper boundary conditions using the FLUENT 6.3.26 CFD software from fluent incorporated.

The simulations was based upon the standard, two-equation $k-\epsilon$ turbulence model of Reynolds Average Navier Stokes (RANs) which is the most appropriate for turbulent flows around an obstacle in a flow path in a channel or pipe flow [4]

3.2 Solver Properties and boundary conditions

Using the fluid properties of water ($\rho = 998.2 \text{ kg/m}^3$, $\mu = 0.001003 \text{ kg/ms}$), the inlet velocity (V), Reynolds number (R), and turbulent intensity were calculated using equations 2, 3 and 4 respectively [3] at flow rates (Q) of 4000 cm^3/s , 5000 cm^3/s and 8000 cm^3/s . The summary of the results of the computation is shown in table 1. In all the cases Since $R_e = > 4000$, flow is a fully developed turbulent flow. [5]

$$V = \frac{Q}{A} \quad (2)$$

$$R_e = \frac{\rho V D}{\mu} \quad (3)$$

$$\text{Turbulent intensity} = \left(\frac{\rho V D}{\mu} \right)^{-1/7} = (R_e)^{-1/7} \quad (4)$$

$$A = \frac{\pi D^2}{4} = 3.142 \times \frac{0.078^2}{4}$$

$$= 4.78^{-3} \text{m}^2$$

$$\text{for } Q = 4000 \frac{\text{cm}^3}{\text{s}}, \quad V = \frac{4^{-3}}{4.78^{-3}} = 0.837 \text{ m/s}$$

$$R_e = \frac{998.2 \times 0.837 \times 0.078}{0.001003}$$

$$= 64973.5$$

$$\text{Turbulent intensity} = \left(\frac{\rho V D}{\mu} \right)^{-1/7} = (R_e)^{-1/7} = 64973.5^{-1/7} = 3.29 \%$$

Table 1: Computed Initial values of velocity, Re and turbulent intensity

Q (cm^3/s)	V (m/s)	R_e	Turbulent Intensity (%)
4000	0.837	64974	3.29
5000	1.046	81,197	3.18
8000	1.674	129,947	2.98

3.3 RANs Modelling parameters

- Order of discretization: 2nd order upwind was used for a better result
- Turbulence specification method: Intensity and hydraulic diameter
- Solver: 2D steady state-pressure based
- Convergence criterion: 1×10^{-6}

3.4 Boundary Conditions:

Two boundary conditions were set in the cause of the initialization.

3.4.1 Inlet boundary condition (velocity inlet)

This is the pipe inlet section. A total boundary condition is imposed there with total pressure set at atmospheric pressure (101325pa) and inlet velocity set as the x-velocity component (values indicated in table 1 for each of the flow rates). The fluid was assumed to enter with negligible vertical velocity component. The flow was assumed to be a fully developed steady turbulent flow. The momentum, turbulent KE and turbulent intensity were set to second order upwind for higher accuracy of results [6]

3.4.2 Outlet boundary condition (pressure outlet)

In the outlet zone, default value for gauge pressure was used because the outlet is to be maintained at atmospheric pressure. Wall zone is set as wall while the adjacent cell zone is set as fluid and the wall is stationary with no slip. The interior and default interior is set as interior.

3.5 Setting of Solution, Initialisation and Residual

In the initialisation, FLUENT was prompted to compute from inlet and initialise for the solution initialisation and under reference frame, absolute was selected.

Iteration was done until the solutions converged. The number of iteration before the solutions converges is shown in table 2.

Table 2. No of iterations for convergence of solution

Type of grid	Flow Rates (cm ³ /s)	Number of Iterations
Coarse	4000	1450
Coarse	5000	1769
Coarse	8000	1740
Fine	4000	4160
Fine	5000	4830
Fine	8000	4106

3.5.1 Pressure measurement point

To evaluate the pressure differences 25mm upstream and downstream of the plate, two iso-planes were created, on the x direction at 202.5mm (upstream) and 257.5mm (downstream).

To simplify the analyses of flow characteristics, more iso planes at 150mm, 400mm, 550mm and 700mm were created along the x-axis called streamat150mm, streamat400mm, streamat550mm, and streamat700mm respectively.

In the y-axis, iso planes at 0mm, 21.5mm that is in-between the plate and the bluff body and at -21.5mm called the centreline, free-stream and bluff-stream respectively were created. It is worthy to note that the origin of y-axis is at the centre of the pipe, which is at supposed 39mm in the y direction. The need of these multiple iso plane is to be able to view the flow properties variations at different section of the pipe, which will make for easy comparison.

4.0 SIMULATION, RESULTS AND DISCUSSIONS

4.1 Pressure difference

Tables 3 and 4 below show simulated results of static and dynamic pressure difference for the different flow rates of the fine grid. It is observed, that the pressure difference increased with increasing flow rate or velocity. This is in agreement with the general principle of dependent of pressure drop to the square of the velocity or flow rate from the bernouli's equation as in equation 1[3] The increase in pressure drop with velocity stems from the fact that at higher velocity, the randomness and rapid fluctuations of the swirling fluid particles called eddies increase throughout the flow. These fluctuations lead to higher rate of mixing and turbulence which give rise to high rate of momentum transfer from the fluid to the pipe walls. This then leads to a higher shear stress and pressure drop.

Table 3: Fine grid Static pressure difference 25mm upstream and downstream for the three flow rates.

Flow rate (cm ³ /s)	V (m/s)	Static Pressure (Pa)		
		P1	P2	P2-P1
4000	0.837	3.5811	19.9956	16.4145
5000	1.046	31.3754	5.4727	25.9027
8000	1.674	82.9684	13.9750	68.9934

Table 4: Fine grid Dynamic pressure difference 25mm upstream and downstream for the three flow rates.

Flow rate (cm ³ /s)	V (m/s)	Dynamic Pressure (Pa)		
		P1	P2	P2-P1
4000	0.837	0.8993	10.9550	10.0557
5000	1.046	1.4036	17.2043	15.8007
8000	1.674	3.5936	44.5887	40.9951

4.2 Comparison of Pressure difference 25mm upstream and downstream for the Coarse and fine grid at 5000 Cm³/s flow Rate

The pressure difference measured 25mm upstream and downstream of the plate for the coarse and fine grids at 5l/s is the same with a negligible deviation of 0.06Pa as in table 5. The result is in agreement with expectation because it is the same fluid, the same flow rate, the same simulation model and the same conditions, the only difference being the difference in grid and mesh which is what accounted for the little difference in the pressure difference calculated.

Table 5: Comparison of the **Static Pressure** difference 25mm upstream and downstream for flow rate of 5l/s using coarse and fine grid

P (Pa)	Coarse grid		Fine Grid	
	Dynamic	Static	dynamic	static
P1	1.39	32.19	1.40	31.38
P2	17.24	6.22	17.20	5.47
P2 -P1	15.85	25.97	15.80	25.91

A. 4.3 Pressure contours

4.3.1 Total pressure

The CFD simulation results showed varying velocity and pressure fields/contours characteristics of turbulent flows. While both pressure drops and flow velocity or pattern along the tube and across the plate vary with flow rates for both the fine and coarse meshes, the flow and pressure contours are closely the same for the three flow rates (4000 cm³/s, 5000 cm³/s, 8000 cm³/s) for coarse and fine grids. Typical total pressure contours for the flow is shown in figures 3, 4 & 5 for 8000 cm³/s flow rate. The contours for the 5l/s and 4l/s bear a close resemblance and are left out here for want of space. At the pipe inlet, the total pressure is uniform (at its maximum) as indicated by the red colour on fig.2. Two vortex zones were formed, one upstream and the other downstream of the plate as indicated in figures 4 and 5. As the fluid approaches the two sharp obstructions in its flow where there is a decrease in the cross-sectional area, the velocity increases, the static pressure decreases and the dynamic pressure increases giving rise to a reduced total pressure as shown by the light blue colour in fig.3. The total pressure reduces continuously across the plate reaching its minimum value at a point immediately after the point of reduced cross-sectional area because of the vortex formed there as indicated in fig.5. Thereafter, the total pressure recovers, increases to a certain value but never to the value before the fluid flow passed through the obstruction. Worthy of note is that the pressure drop across the plate increases along the length of the pipe between 25mm upstream and 25mm downstream of the plate because of increase in resistance as a result of velocity increase along the length

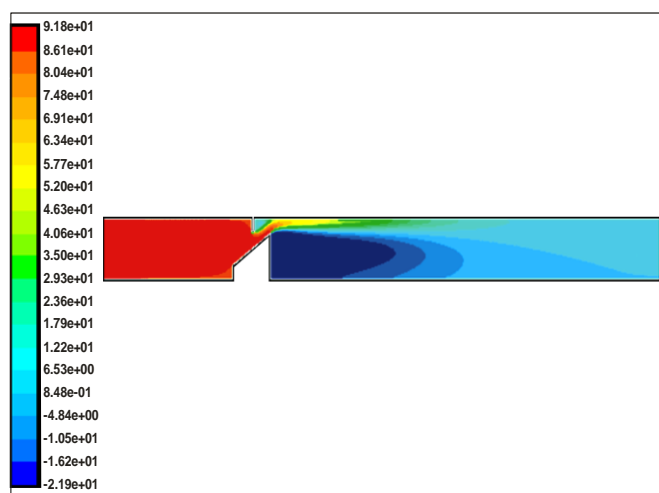


Fig 2: Contours of Total pressure

4.3.2 Static and dynamic Pressure

From the contours of static pressure from the CFD simulation, it is observed that the static pressure is maximum at the inlet and decreases as the fluid approaches and passes through the reduced cross-sectional area (as shown by the red and yellow colour of fig.3). This is because of increase in velocity at that point as a result of reduction of cross-sectional area. As the fluid passes through the reduced cross-sectional area, the static pressure decreases reaching its minimum value at a point just after the reduced area section downstream corresponding to the point where vortex was formed in the velocity stream lines and contours (see blue colour of fig.6). Thereafter, the static pressure recovers, increases slightly above the minimum value reached (see light blue colour of fig.3).

The dynamic pressure on the other hand was at its minimum at the inlet, increased as the fluid passes through the area of reduced cross-section, then reaching its maximum at the minimum cross-sectional area corresponding to the point of maximum velocity reached in the velocity contours. (see red and yellow colour of fig.4). Thereafter, dynamic pressure reduces until it gets to its initial value at the exit corresponding to the initial value at the inlet as shown by dark blue colour of fig.4.

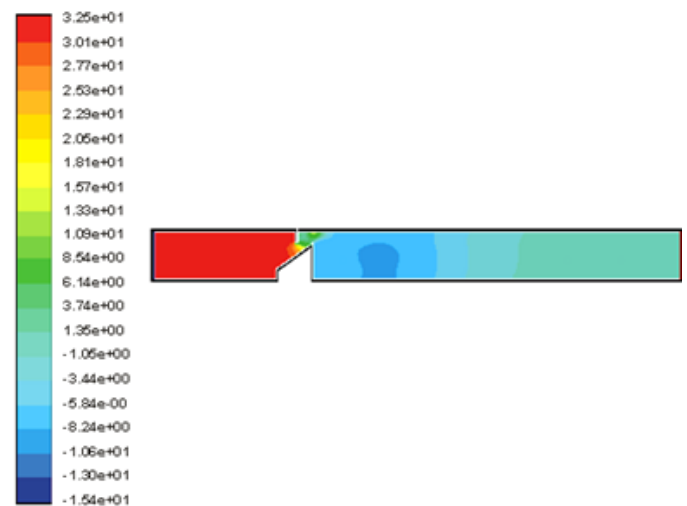


Fig 3: Contours of static pressure

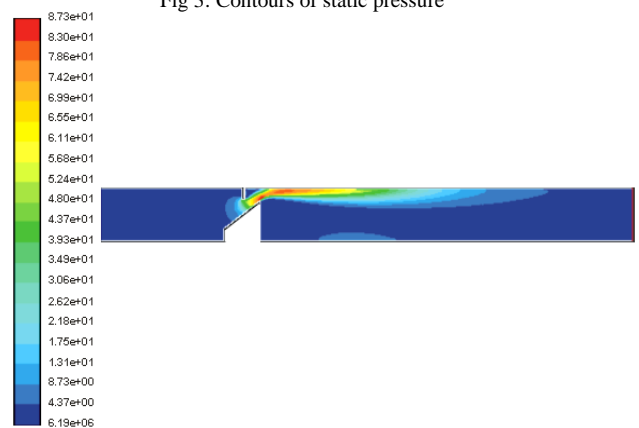


Fig 4 Contours of dynamic pressure

6.1 Velocity distribution

Typical velocity contour of the flow for 5000 cm³/s flow rate is shown in fig .5

The flow being a turbulent flow is characterised by unsteady eddying motions that are in constant motion with respect to each other. Two sets of vortices were developed, one at the upstream of the plate and the other at the downstream as shown by the label in figure 5. Figures 5 and 6 show the velocity distribution in the horizontal iso planes in the pipe: at the centre, between the plate and bluff (21.5mm) and at -21.5mm. It shows that the maximum velocity in the freestream line does not occur exactly in-between the plate and bluff which has the smallest geometrical area, but occurs at about 250 to 260mm (about 20mm from the smallest geometrical area), this point (250-260mm) is the smallest active flow area in that horizontal line as can be observed in figure 8. The outlet velocity seen in the horizontal iso planes of figures 5 and 6 conform with the observation in the vertical iso plane as discussed above that the outlet velocity is not uniform across the outlet but decreases down the pipe slightly in the vertical axis. The negative values of the x velocity plots indicate back flow.

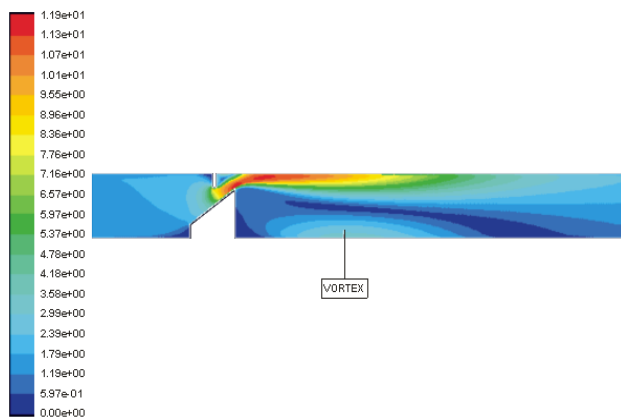


Fig 5: Contours of Velocity magnitude for fine mesh (5l/s flow rate)

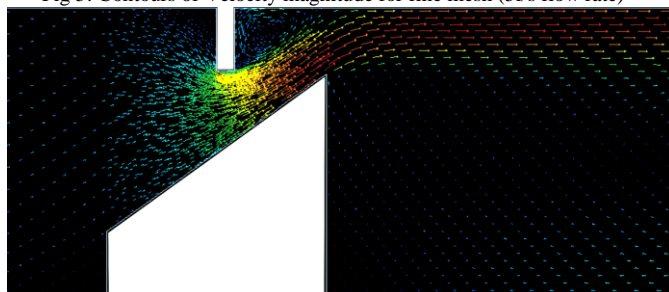


Fig.6 Enlarged view of contours of velocity magnitude for fine mesh (5l/s flow rate)

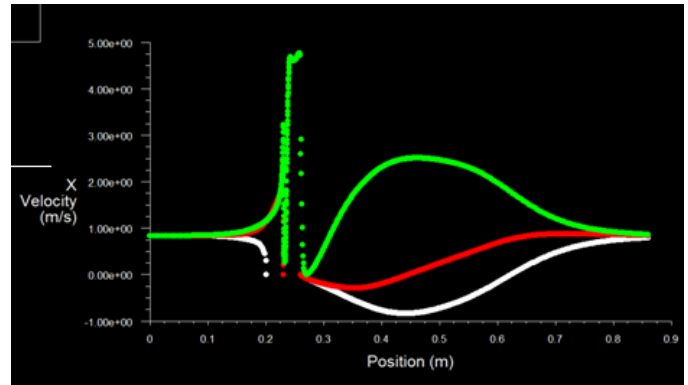


Fig 7 The x-axis velocity profiles (horizontal iso planes) of streams at 21.5mm(white), centerline(red) and -21.5mm(green) for fine mesh (5l/s flow rate)

Velocity streamlines in fig. 8 depicts the mass flow rate from inlet through the outlet. The mass conversation principles tell us that the highest mass flow rate value should occur at the smallest area of flow geometry (tip of the bluff), but discretely the highest mass flow rate is not at the tip of the bluff but it is at the plate section which is about 1 mm bigger than the actual smallest flow section.

Velocity streamlines in fig. 8 depicts the mass flow rate from inlet through outlet. The mass conversation principles tell us that the highest mass flow rate value should occur at the smallest area of flow geometry, but discretely the highest mass flow rate is not at smallest area but it is at a zone in-between the plate and the tip of bluff section.

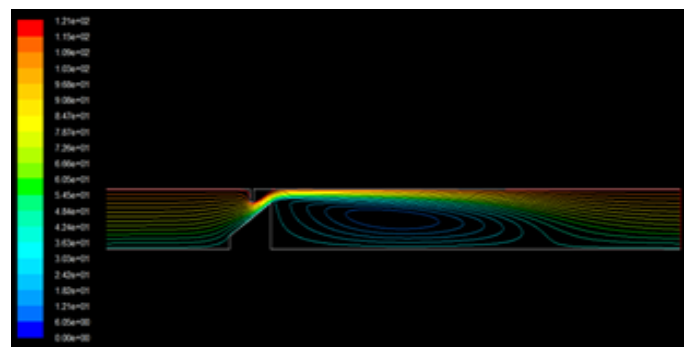


Figure 8 Contours of stream functions for fine mesh at 5l/s

5. CONCLUSION

The results obtained from the simulation of the turbulent pipe flow are in agreement with theory. These results indicated that the pressure difference is proportional to the flow rate or velocity. The velocity of the fluid increased continuously across the plate from 25mm downstream to 25mm upstream. The pressure differences (static, dynamic and total) calculated for both the fine and coarse grid indicate that there is pressure drop in total, absolute and static pressures, while the dynamic pressure will increase across the plate. The result conforms to analytical representation of energy conservation from Bernoulli equation and continuity equation.

On velocity and pressure flow patterns the simulated results for the flow rates ($4000 \text{ cm}^3/\text{s}$, $5000 \text{ cm}^3/\text{s}$ & $8000 \text{ cm}^3/\text{s}$) for both the coarse and fine grids showed similar flow patterns. Two vortices were formed, one at the entrance to the region of the reduced cross-section and the other located just after the reduced cross-section zone downstream. These vortices produced two zones of low pressure that greatly enhanced the total pressure loss across the plate. Also analysis of the velocity stream lines revealed two recirculation zones, one upstream very close to the plate and the other downstream.

Because there is a reduction in flow cross sectional area across the plate, there was a continuous increase in flow rate and hence velocity along the section. This increased the flow resistance giving rise to continuous pressure drop between 25mm upstream and downstream of the plate.

An attempt was made to refine the meshes and observe the simulated results; it was observed that an increase in mesh refinement could likely enhance the features of the flow patterns and contours; but the overall results for the two grids are not very different from one another, thus indicating that the result obtained on the meshes are grid –independent to a high

level of accuracy and additional mesh refinement at an huge cost is not necessary.

REFERENCES

- [1] G.K Batchelor, “*An Introduction to Fluid Dynamics*” Cambridge University Press, Cambridge. 2000
- [2] A. Paul and M. Gorazd “*Fluid Dynamics with a Computational Perspective*” Cambridge University press, London , 2007.
- [3] M. Frank White “*Fluid Mechanics*” 5th ed., McGraw-Hill, New York 2003.
- [4] M.B Abboth and D.R Basco “*Computational Fluid Dynamics; an introduction for Engineers*” Longman Scientific & Technical, New York 1994
- [5] Yunus Cengel and John Cimbala “*Fluid Mechanics Fundamentals and Applications*, 3rd Ed. McGraw-Hill, New York 2013
- [6] Fluent Inc, “*FLUENT 6.3 Tutorial Guide*” (September 2006